36th AIAA Fluid Dynamics Conference and Exhibit
5 - 8 June 2006, San Francisco, California

AIAA 2006-2865

Direct Measurements of the Kinematics and Dynamics of Bat Flight

Xiaodong Tian[*], Jose Iriarte[†], Kevin Middleton[‡], Ricardo Galvao[#], Emily Israeli[#], Abigail Roemer[&], Allyce Sullivan[&], Arnold Song[§], Sharon Swartz[**] and Kenneth Breuer[††]
Brown University, Providence, RI 02912

Experimental measurements on the flight of bats are presented. High speed stereo kinematic motion during straight and turning flight, as well as measurements of the wake velocity field behind the bat are presented. The kinematic data reveals that, at the relatively slow flight speeds considered, that the wing motion is quite complex, including a sharp retraction of the wing during the upstroke and a broad sweep of the fully extended wing during the downstroke. The data also indicates that the bat flight speed and elevation are not constant but oscillate, synchronized with the movement of the wing in both the horizontal and vertical planes. PIV measurements in the transverse (Treffz) plane of the wake velocities indicate a complex wake vortex structure dominated by a strong wingtip vortex shed from either the wing tip (during the downstroke) and perhaps from more proximal joint during the upstroke. Data synthesis of several discrete realizations suggest a "cartoon" of the wake structure during the entire wing beat cycle although a considerable amount of work remains to be done to confirm and amplify on these results.

Nomenclature

A	=	amplitude of the wingtip movement
b	=	half-span of the bat
c	=	wing chord of the bat
f	=	wing beat frequency
L	=	lift per unit span
Re	=	Reynolds number, Uc/ν
St	=	Strouhal number, fA/U
t	=	time
T	=	wing flapping period
u	=	forward flight speed of bat
U	=	mean forward speed
w	=	vertical speed of bat
x	=	streamwise coordinate, positive is in the direction of flight
y	=	transverse coordinate, positive is from the center of mass to the bat's left
z	=	vertical coordinate, positive is up
ν	=	kinematic viscosity of air
ρ	=	air density
Γ	=	vortex circulation

[*] Postdoctoral Researcher, Division of Engineering
[†] Graduate Student, Department of Ecology and Evolutionary Biology
[‡] Postdoctoral Researcher, Department of Ecology and Evolutionary Biology
[#] Undergraduate Student, Division of Engineering
[&] Undergraduate Student, Department of Ecology and Evolutionary Biology
[§] Graduate Student, Division of Engineering.
[**] Associate Professor, Department of Ecology and Evolutionary Biology
[††] Associate Professor, Division of Engineering, Engineering, Box D, Brown University, Providence RI 02912. Tel: 401.863.2870; (fax) 401.863.9028; Email: kbreuer@brown.edu (Corresponding Author)

I. Introduction

ALTHOUGH the tools for the analysis and design of vehicles optimized for steady flight are well developed, there remains a great deal of uncertainty regarding the mechanics of highly unsteady flight. This is an issue of growing interest, driven by the desire to build vehicles that can perform extreme unsteady aerodynamic maneuvers. As engineering materials, actuators and controls have become more sophisticated, we are able to think about mimicking the natural world. Such efforts, however, have been hampered by the lack of development of actuators for biomimetic flight, and at a more fundamental level, by deep gaps in our understanding of the basic mechanics of the highly unsteady, three-dimensional and complex character of animal flight. Flapping flight is the single most evolutionarily successful mode of animal locomotion: there are today over 1,200 species of bats, more than 10,000 living species of flying birds, and somewhere between millions and tens of millions of species of flying insects. Understanding how animals fly is not only central to providing insight into the biological world; the rich diversity of mechanisms of animal flight can provide abundant inspiration for engineered design.

It is therefore surprising that decades of research into the biology of bats, birds, and insects have been conducted without much understanding of the mechanistic basic of animal flight. With few exceptions, it is only in the last twenty years that biologists have begun to rigorously address this knowledge gap. Recently, however, application of fluid dynamic approaches has revolutionized understanding of insect flight. Computational fluid dynamics, detailed force measurements from tethered animals, and physical modeling of wake structure, using both smoke visualization and particle image velocimetry (PIV), have been integrated to reveal mechanisms responsible for the generation of aerodynamic forces in insects to a degree previously almost unimaginable. A review that includes many recent works on the aerodynamics of insect flight can be found in Sane[1]. Detailed fluid dynamics approaches are now being applied to the study of bird flight as well (Spedding[2], Warrick[3]). The velocity fields in wake flows generated by birds have been measured using PIV. These studies on birds demonstrate that it is possible to analyze the structure of the flow in the wakes of flying vertebrates, and to calculate mechanical and energetic quantities directly from the wake 'footprint'.

Although biologists and engineers have begun to scratch the surface of insect and bird aeromechanics, studies of flight in bats have yet to make comparable progress. Most investigations of vertebrate flight have assumed that animal aerodynamics can be meaningfully approximated by assuming that bat and bird wings function in the same way as rigid, fixed wings of large, fast, human-engineered aircraft. On this basis, a large biological literature attempts to infer maneuverability, flight energetic, and other aspects of flight performance and ecology from simple metrics such as aspect ratio and wing loading. Although this simple approach is a reasonable place to start a quantitative analysis of animal flight, it is clearly too simplistic. In contrast to most fixed-wing aerodynamics, bats fly at low Reynolds number (10^4–10^5), have highly compliant aerodynamic surfaces and are characterized by highly unsteady and three dimensional wing motions (Fig. 1). Their multiply jointed wing skeleton, thin elastic wing membrane and several other morphological features enable these animals to exhibit extraordinary flight performance. These features must be considered when trying to understand the complexity of bat flight. In particular, bats differ from all other flying animals in the complex functional mechanics and architecture of wings, physiological energetic of locomotion, and the kinematics and maneuverability of flight. These facts together suggest that the study of bat flight can be rich and productive, and lead to insights distinct from those gained through study of flight in other animals.

In this paper we present initial experimental data from a research program motivated by the following fundamental questions:

a) What are the aerodynamic capabilities of bats – how do they differ from that of birds and insects? What are the quantitative aerodynamic metrics by which we can measure the animals' performance?

b) We know that bats have several morphological and physiological features that are unique in the animal kingdom. What are the roles, if any, of these different features in the observed aerodynamic capabilities of bats?

c) How can we model the aeromechanical behavior of the bat so that might guide engineered vehicles that take advantage of bats' capabilities?

The data presented in this paper will be a small step trying to address primarily questions (a) and to some extent (b). We have conducted flight cage experiments with live bats and have measured their detailed kinematic motion. In addition, using PIV, we have made measurements of the wake velocity structure behind the animal as she flies down the flight cage.

Figure 1 A bat (*Cynopterus brachyotis*) in flight. *(a) Beginning of downstroke, head forward, tail backward, the whole body is stretched and lined up in a straight line. (b) Middle of downstroke, the wing is highly cambered. (c) End of downstorke (also beginning of upstroke), the wing is still cambered. A large part of the wing is in front of the head and the wing is going to be withdrawn to its body. (d) Middle of upstroke, the wing is folded towards the body.*

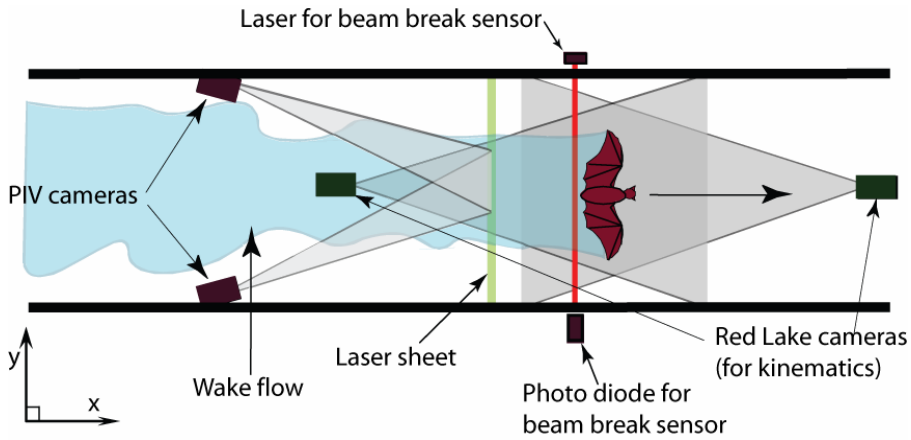

(a) Top View

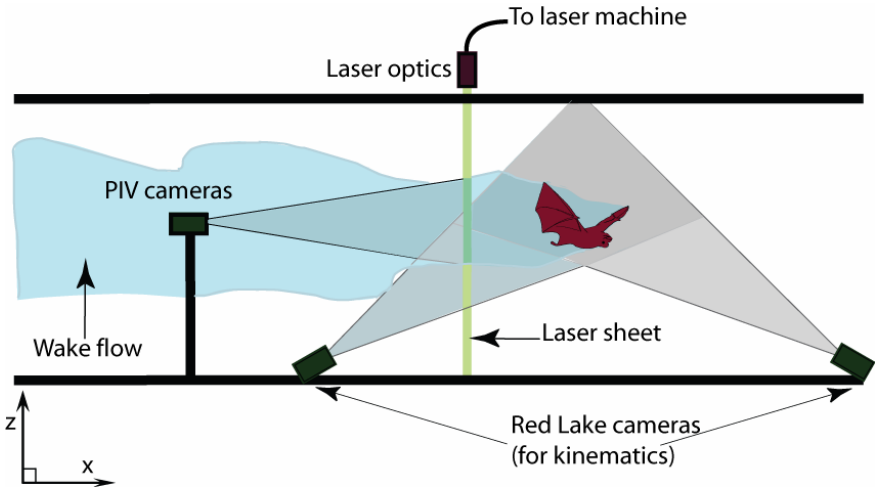

(b) Side View

Figure 2 Schematic of the experimental setup for the measurement in the transverse (Trefftz) plane. *The bat flies from left to right and triggers the acquisition sequence by triggering a beam-break sensor. The wake is imaged in a plane behind the animal, after she has passed through.*

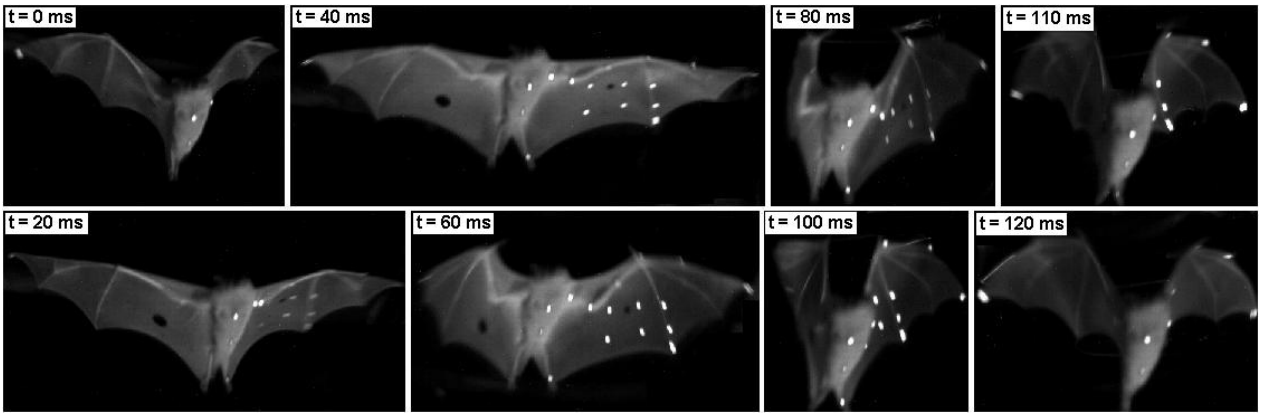

Figure 3 Sequences of images from one high speed video cameras mounted on the test section floor. *The bat is flying towards us. The shoulder, sternum, hip bone, and one wing have been marked with reflective markers. These markers are clearly seen when the wing is fully open. During the downstroke, the wing is fully open and stretched out to get maximum lift. During the upstroke, the substantial bending of elbow, wrist, and finger joints is evident.*

II. Experimental Setup

All experiments were performed in an enclosed flight cage located at the Concord Field Station of Harvard University. The flight cage is 8 m long with a cross sectional area of approximately 1 m (width) × 2 m (height). Lesser short-nosed fruit bats, *Cynopterus brachyotis*, were the subjects of all tests. Native to many forested areas of Southeast Asia, 20 captive-bred individuals have been loaned to us by the Lubee Bat Conservancy, a bat research and conservation organization based in Gainesville, Florida. All bats are female, eliminating any variation due to differences between the sexes. Four were selected as test subjects based on their consistent flight behavior and cooperation during training sessions and experiments. Previous studies have found that the forward flight speed of bats vary with body size and mass across species (Winter[4]). In the flight cage, the average forward speed of bats range from 2 to 3 m/s, somewhat slower than their preferred flight open range flight speed. The animals used in this study had a body mass of approximately 40 grams and wingspans of approximately 40 cm.

A top view and a side view of the experimental setup are illustrated in Fig 2. The bat flies through the flight cage (from left to right). Her body and wing movements are captured by a pair of Redlake high-speed, low-light sensitive video cameras (MotionScope PCI 1000, operating, at frame rate 500 s^{-1}). Both cameras are positioned on the floor looking upwards with advancing and receding angles. The twin camera arrangement allows for the acquisition of the complete three-dimensional motion of the bat. Low light conditions were preferred because the bats are nocturnal and PIV measurements require a reduced light condition. As the bat flies through the flight cage, it trips a laser beam-break sensor which initiates the data acquisition sequence. After a pre-set delay (typically 300 ms, calculated to allow the bat to pass through the measurement volume) the wake flow is illuminated by a sequence of laser pulses using a pair of Nd:YAG lasers (5 ns, 150 mJ/pulse, typically 1000 μs between adjacent images, 200 ms between adjacent image pairs). The laser beam is guided through a series of optics and finally spread out as a laser sheet from the flight cage ceiling. The test section is seeded with a light mist of micron-sized aerosol particles generated by a custom-built Laskin nozzle fog generator (Kähler[4]). The motion of the tracer particles is captured by a pair of high-resolution CCD cameras (LaVision FlowMaster3 system, image size 1376×1040). Both PIV cameras are mounted on a frame and their heights are adjusted at the level of the bat's flight. The velocity field is then extracted using standard 3D stereo PIV procedures from the pair of images (using LaVision PIV software). By piecing together several image pairs captured from the wake as a function of time, a complete portrait of the wake flow behind the animal can be acquired.

As shown in Fig. 2, the x-axis is defined as the bat's flight direction, the y-axis is the transverse direction toward to the bat's left, and the z-axis is the vertical direction. The origin of the coordinate system is defined as the point where the bat's sternum (approximately its center of mass) passes through the laser sheet.

III. Results and Discussions

A. Straight Flight Kinematics

Fig. 3 shows eight images taken from one of the high-speed camera sequences. The bat has been marked using reflective tags to key locations on the bats body and some of the wing joints. The sequences record one whole wing beat. From the video record, one can clearly see the highly articulated motion of the bat, in complete contrast to the relatively simple flapping motion of the birds and insects. More than two dozens independently controlled joints in the wing (Swartz[5], Vaughan[6]) and highly deforming bones (Swartz[7-9]) enable the bat to fly at either positive or negative angle of attack, dynamically change wing camber, and create complex 3D wing topology to achieve extraordinary flight performance. Post processing of the high speed videos (using custom written MATLAB software) yields the unsteady three-dimensional motion of the entire wing-body system. Fig. 4 shows one example of such a result on wingtip movements relative to the sternum. The red symbols are those measured from the stereo video record while the green symbols on the orbit indicate points that have been interpolated due to obstruction of the marker point. The top view indicates that the wingtip outlines a circle during the downstroke, similar to that of birds and insects. During upstroke, however, the wingtip path is a complex curve. The wingtip is first brought very close to the body. It is then extended away from the body, and at the end of the upstroke it is slightly moved toward the body again. The side view shows the wingtip moves diagonally from behind the sternum toward the head and from above the sternum to below the sternum during downstroke. The wingtip position is above the sternum for the majority of the wing beat. Both views show the wingtip position changes more abruptly as the bat begins the downstroke and starts to extend the wing away from the body. The transverse path of the wingtip is smoother during both the downstroke and upstroke than the vertical path because the digitizing uncertainty in vertical direction is higher.

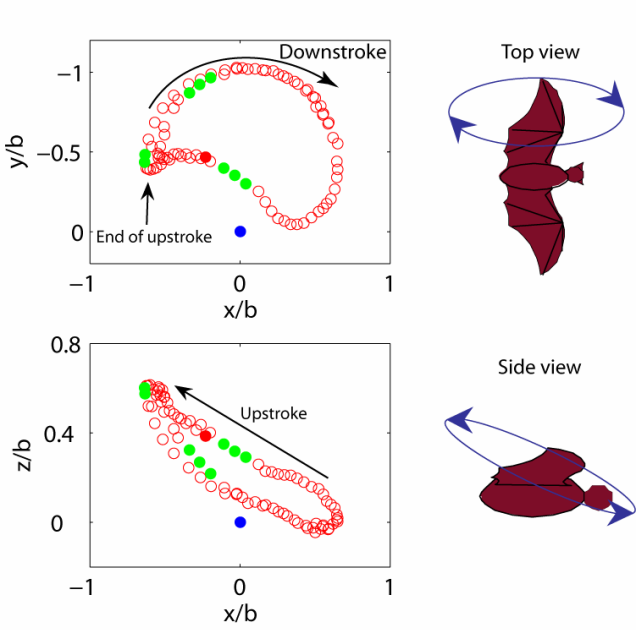

Figure 4 An example of wing tip motion. *Shown are a top view (streamwise versus transverse position) and side view (streamwise versus vertical position) of the left wingtip position for a single run, and a diagrammatic depiction of the wingtip motion represented by the plots. The red circles indicate the data obtained from reflective markers. The green dots are data by interpolating because of the markers are not visible. The blue dots represent the position of the sternum. The diagrams of the bat represent the related position and direction of movement of the wingtip shown in the plots.*

The time course of typical wing tip movement relative to the center of mass is shown in Fig. 5a. Fig. 5b shows the bat's flight speeds in forward and vertical directions. The original data obtained from videos are sternum positions varying with time. The flight speeds are calculated by taking the derivative of the sternum position. The derivative is calculated by fitting a quadratic polynomial using a local template (a size of 15 points was selected in this paper.)

The wingbeat frequency and amplitude were derived from fitting a harmonic sine series to the wingtip positions:

$$F(t) = C + Bt + \sum_{i=1}^{N} A_i \sin(i\varpi\ t + \phi_i) \tag{1}$$

where F is the overall wing tip position, C and B are two constants representing the linear trend (for example if the animal is ascending or descending during the acquisition), t is time, N is the number of Fourier modes, A_i is amplitude of each mode, ϖ is the wing flapping frequency $f = \frac{\varpi}{2\pi}$, and ϕ is the phase offset. Note that a single frequency is used for all the Fourier modes although each mode is allowed a unique amplitude and phase. The optimal number of Fourier modes, N, was determined by fitting errors. The error was defined as the root-mean-

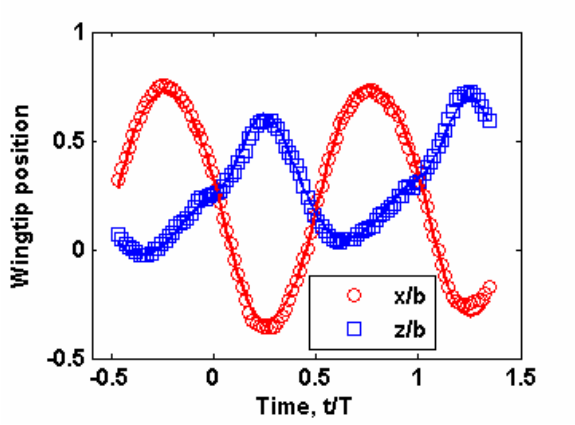

(a) Wingtip positions

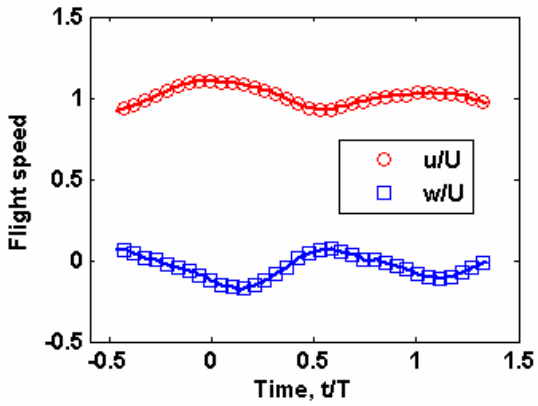

(b) Flight speeds of the bat

Figure 5 Typical kinematics from bat flight measurements. *The left frame shows vertical and forward wing tip positions relative to the center of mass while the right frame shows the bat flight vertical and forward speeds. The red circles and blue squares are the original data. The solid lines are fitting lines based on Eq. 1.* We're missing units on the y axes-

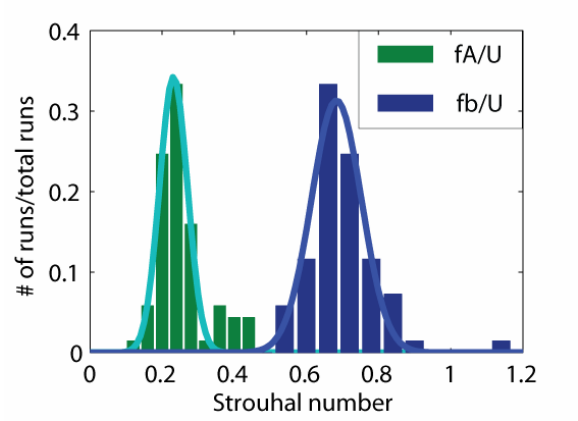

Figure 6 Strouhal numbers, *calculated from the kinematic data based on the vertical wingtip amplitude and half wingspan, respectively. fA/U is centered around 0.25 which falls within the range of 0.2 < St < 0.4 given by Taylor et al[10] for cruising flight. fb/U is centered around 0.7, which means in every wingbeat the bat flies a distance of b/0.7.*

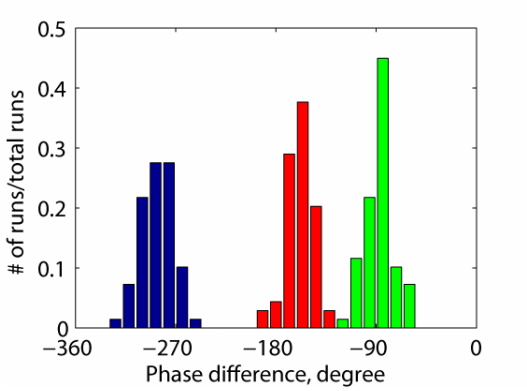

Figure 7 Phase relationships. *Wing tip vertical movement (red), vertical flight speed (blue), and forward flight speed (green), all relative to the wing tip horizontal movement. The phase shift in wing tip vertical movement is about -180 degrees. It is -90 degrees and -270 degrees in the forward speed and vertical speed, respectively.*

square deviation between the experimental data and the analytical fit. Typically, this error decreased from approximately 5% of the peak-to-peak amplitude ($N = 1$) to less than 1% ($N > 4$). $N = 4$ was used for all fitting presented here.

Using this technique, wing beat frequencies ranged between 7.8 Hz and 10.2 Hz over a total of 67 runs, with an average of 8.81±0.45 Hz. The Strouhal number is often used to describe the wing kinematics of flying animals:

$$St = \frac{fA}{U} \quad \text{or} \quad St = \frac{fb}{U} \tag{2}$$

where St is Strouhal number, A is amplitude of the wing tip vertical movement which is a half of the distance between the lowest and highest wing tip position, b is the half wingspan, U is mean forward speed. Fig. 6 shows the histogram of Strouhal number. The Strouhal number based on wing amplitude, fA/U, ranges from 0.14 to 0.44 with a mean value is 0.25±0.07. The Strouhal number based on half-span, fb/U, ranges from 0.54 to 1.17 with a mean

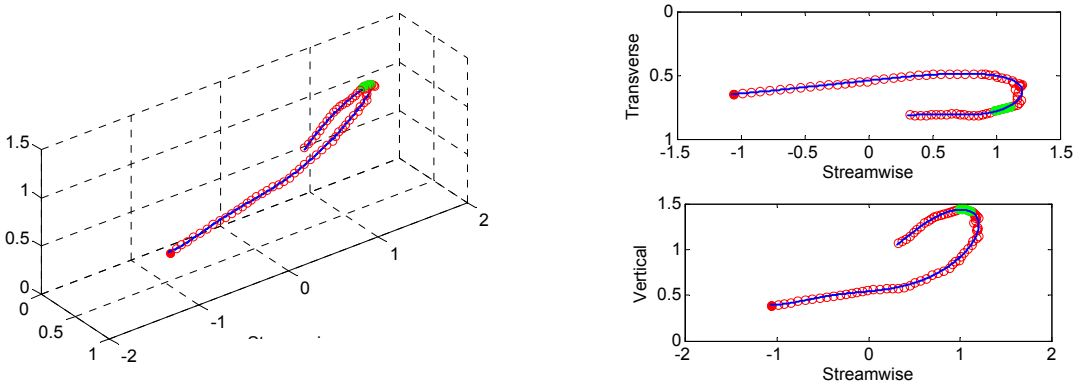

Figure 8 Turning kinematics. *The left frame shows the location of the sternum during a 180 degree turn. The bat flies in from the left, rises, turns and flies out again. Views from the top and the side are shown on the right side, in the upper and lower frames respectively. Red symbols indicate every 5th data point, green circles are interpolated points where the sternum marker was obstructed from one or both of the camera views.*

value is 0.7±0.09. All bats used in the tests have been trained to fly straight and fly from one end of the flight cage to the other end. During experiments, however, the bat sometimes flew slightly up to the ceiling or turned to the side walls. Both the wing flapping motions and flight speeds change when the bat prepares a turn or a stop. The wingtip movements and wingbeat frequency also vary between individual bats. The effects of these variations are beyond the scope of the current paper.

Fig. 5 illustrates that while the bat flight speed is not constant, it is clearly synchronized with the wing motion. The wing motion in the horizontal plane is largely sinusoidal. However the tip motion in the vertical plane (z) illustrates a higher harmonic of some strength, contributing to the "kink" in the motion during the upstroke (when the animal retracts its wings). The lift or thrust force generated by the wing flapping must have the similar periodic variations. Using simple dynamics, we know that a motion generated by a sinusoidal force will exhibit a velocity 90 degree out of phase with the force. This is confirmed in Fig. 7, which shows histograms of phase differences (referenced to the horizontal wing tip motion) of the animal's velocities and wing tip vertical displacement. Consistent with figure 5, we see that the vertical tip movement (red) is 180 degrees out of phase with the horizontal movement. In addition the vertical flight speed (blue) appears to lag the horizontal wing movement by 270 degrees, or more intuitively, to lag the vertical wing displacement by 90 degrees. Similarly, the axial speed (green) lags the horizontal movement by 90 degrees.

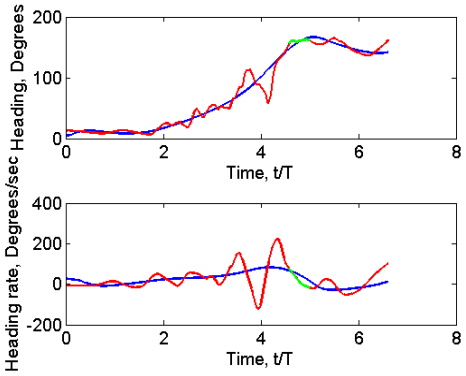

Figure 9 Heading and heading rate during 180 degree turn. *Heading is the angle between the bat flight direction and the forward x-direction. Heading rate is the change of the heading, calculated from the heading data.*

B. Turning Kinematics

We have also acquired some preliminary kinematics for 180 degree turns. Bats are extraordinarily agile, and these measurements represent some of the first detailed measurements of bats during these extreme maneuvers.
Fig. 8 shows the trajectory of the bat's center of mass during a 180 degree turn. The raw marker positions are shown in the three coordinate axes. As before, green symbols indicate the points that have been interpolated due to marker obstruction. From a purely aerodynamic perspective, the performance of this turn is very impressive. The bat flies in and turns back in a very narrow space (less than a half of its wing span) and accomplishes the turn within three wing beats (T = 2-5). In order to do this, she rises, turns and drops back down as she flies out in the opposite direction, regaining her incoming velocity almost immediately. Fig. 9 shows the bat heading and heading rate during the 180 degree turn. When t/T is greater than 2, the heading slowly changes and the bat prepares for a turn. After t/T = 3.5, the heading increases in a faster rate and the bat finishes the turn after t/T = 5. The major part of the turn is finished in less than 2 wing beats.

C. PIV Data Analysis

Fig. 10 shows a series of wake velocity fields from the transverse (*Trefftz*) plane. The measurement plane is on the left side of the bat, with the coordinate origin centered on the position of the sternum as it pieced the PIV imaging plane. It is evident that there is a strong wing tip vortex generated by the bats flight. The vortex decays in strength, and advects downwards. Since the vortex is well defined, the vorticity can be determined based on Stokes' theorem from calculation of the circulation, Γ, via contour integration normalized by the area enclosed by the contour composed of differential elements $d\mathbf{r}$[11]:

$$\int \boldsymbol{\omega} \cdot \mathbf{n}\, dA = \oint \mathbf{u} \cdot d\mathbf{r} \tag{3}$$

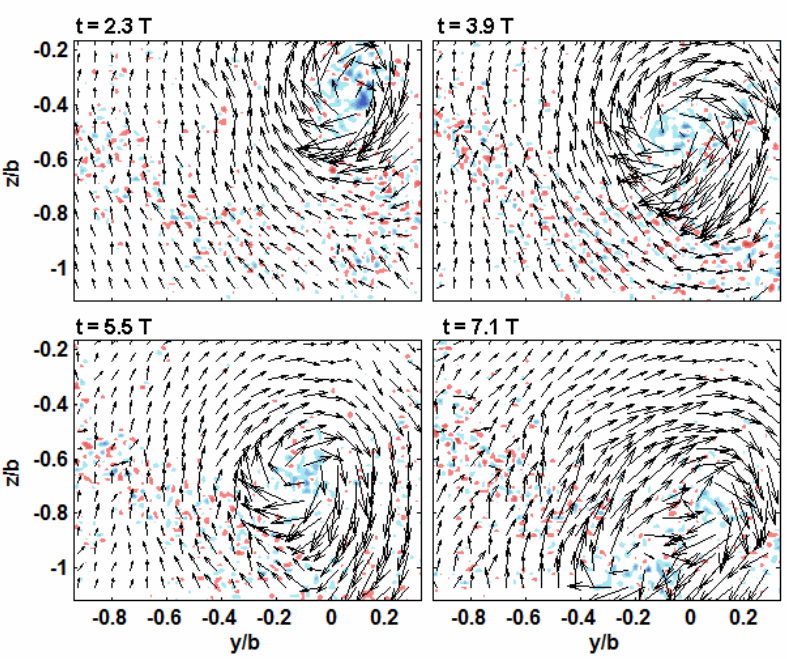

Figure10 Typical wake velocity fields from PIV images. *The origin (y/b=0, z/b=0) is the point where the center of mass pierced the PIV plane. For this case, the bat passed above the PIV plane. The background of each frame is vorticity field. The darker the color, the stronger is the vorticity. Blue indicates positive vorticity and red indicates negative voticity. There is a 200 ms separation between successive PIV images.*

The integration is performed along the edges of 1x1 square interrogation windows using the velocity values at the square's vertices. This vorticity calculation is performed with no oversampling of the interrogation windows. This method is used to attenuate the effects of measurement noise on the vorticity field by employing more points for its calculation[12].

The majority of the flow fields measured in this series of experiments exhibit a complexity which makes the task of defining the vortex core difficult. As shown in Fig. 10, within the main core itself, there exist smaller vortical structures of opposing vector directions. Therefore one cannot simply define the vortex cores as connected regions of vorticity of the same sign. Thus, an alternative method of defining the vortex core was devised to accommodate these nuanced structures so that the circulation could be estimated from these data.

The circulation was only calculated for data similar to Fig. 10 where it was visually apparent that a vortex was located in the measurement plane. According to Eq. (3), the circulation of a region can be calculated by integration of the velocity along the contour that is the boundary of this region. For simplicity, this analysis employed circular contours in the circulation calculations. To find the "center" of the vortex core a rectangular region was manually selected, via visual inspection, with care taken to enclose the majority of the main flow structure. The centroid of vorticity within this rectangular interrogation window was then calculate and was defined as the "center" of the vortex core. This location served as the point about which a series of integrations about concentric circular contours of increasing radii were performed to determine the magnitude of the circulation as a function of area enclosed. Utilizing the condition that the flow outside of the vortex core is irrotational, the vortex core was defined to be the region within which the circulation reaches a maximum (Fig. 11). Although the flight is clearly unsteady, we can use the Kutta-Joukowski theorem for steady flight as an estimate of the lift per unit span[13]:

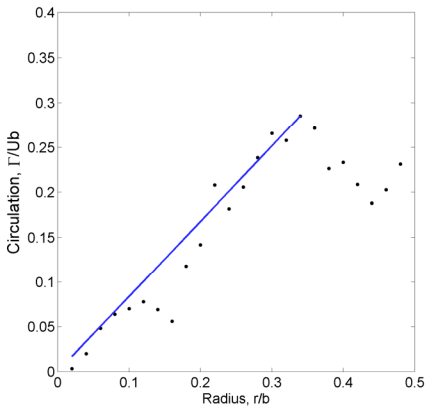

Figure 11 Circulation inside tip vortex. *The circulation rises through the vortex core before reaching an approximately constant value of 0.25.*

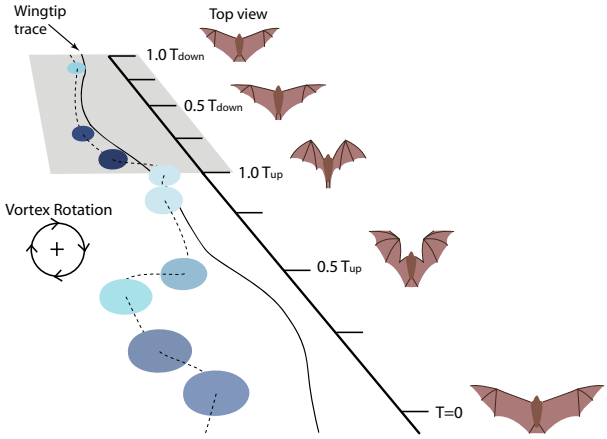

Figure 12 Schematic reconstruction of wake geometry. *Wake images are at constant distance downstream of the bat. The darker the vortex color, the stronger is the vorticity.*

$$L = \rho U \Gamma \tag{4}$$

Where L is lift per unit span, ρ is air density. Based on the maximum circulation calculated here, the total lift can be approximately estimated as 0.24 N, which, at the measured flight speed (2 m/s) should be able to support a mass of 25 gram. This is comparable to, but underestimates, the measured mass (~40g), but is, at least, in the right neighborhood, considering the simplicity of this argument. Clearly more detailed measures of the circulation and its relationship to the true momentum balance need to be performed, although this is not possible with the slow rate of velocity field acquisition (5Hz, or every two wing beats) that was available to us for this first set of experiments.

Each PIV acquisition sequence is, however, accompanied by the complete kinematic history of the flight. This enables features identified in the wake structure to be associated with specific wing/body motions. It is a challenge to couple the PIV and 3D kinematic data because runs differ in flight speed and trajectory. To achieve meaningful data synthesis, we first adjust the coordinate origin and normalize velocity. As mentioned earlier, the coordinate origin is defined as the point where the center of mass passes the PIV plane. The velocity field is then non-dimensionalized by the flight speed associated with each particular acquisition. Each run is then rearranged and collated based on the wing beat phase angle. In this manner, we are able to determine the location of the vortex core relative to the bat as well as the relative wing location with respect to the wingbeat cycle as it moves through the PIV plane. Accordingly, we can reconstruct a "cartoon" of the wake shed by the bat as it moves through its wingbeat. Our first attempt at this reconstruction is shown in Fig. 12, although it should be emphasized that this is hindered by a rather small set of realizations available in the ensemble. The main trailing vortex structures deposited by the bat on the downstroke closely follow the wingtip trace as one might expect. But, in the case of the upstroke the vortices shed appear to fall outside of the wingtip trace. On the upstroke, the animal folds its wings in towards the body to the point where the wingtips may no longer be the outermost extension of the bat. Therefore, the wake pattern suggests that these upstroke vortices are most likely shed from another location along the folded wing, possibly the wrist joint. More work is needed to validate and to amplify on this proposed wake pattern.

IV. Conclusions

Experiments have been performed to capture the coupled kinematics and wake velocities of bats. The kinematics data reveal that, at the relatively low flight speeds considered here, that the bat has unique (I think 'rather unique' is like 'somewhat pregnant'!) flight characteristics, quite distinct from those observed in both insect and vertebrate flight, including a quite dramatic drawing-in of the wing during the upstroke compared to the fully-extended sweep that characterizes the downstroke. In some respects it is almost like the animal is "rowing" rather than flying! Measurements have also characterized maneuvering flight, in particular a 180 degree turn which the bat executes in an extraordinarily compact and fast manner, exhibiting turn rates exceeding 200 degrees/sec. The

kinematic data also show that the bat flight speed and elevation are not constant, but are closely synchronized with wing horizontal and vertical motion. The PIV data, though preliminary, indicate strong wing vortices and a complex vortical wake structure, although these need to be verified and explored further. Preliminary wake geometry is successfully reconstructed.

The experiments presented in this paper represent the first detailed measurements on both kinematics and wake velocities of bats and while encouraging, are still lacking in both quantity and quality. Improvements in the equipment (higher resolution high-speed cameras, higher frequency PIV system, etc.) are currently being implemented, and further experiments will yield more insights into the abilities and underlying biomechanics that these animals exhibit.

Acknowledgments

All experiments were conducted at the Concord Field Station (CFS) at Harvard University and we express our thanks to the CFS staff, especially Andy Biewener, the director of CFS, for his support. We are also most grateful to Dr Ty Hedrick for his assistance, and for the use of his kinematics digitizing code. The work is supported by the Air Force Office of Scientific Research (AFOSR), monitored by Dr. R. Jeffries and W. Larkin, NSF, and the Brown University UTRA program.

References

[1]Sane, S.P., "The aerodynamics of insect flight," *The Journal of Experimental Biology*, Vol. 206, 2003, pp. 4191-4208.

[2]Spedding, G.R, Hedenstron, A., and Rosen, M., "A family of vortex wakes generated by a thrush nightinggale in free flight over its entire range of flight speeds," *The Journal of Experimental Biology*, Vol. 206, 2003, pp. 2313-2344.

[3]Warrick, D.R., Tobalske, B.W., and Powers, D.R., "Aerodynamics of the hovering hummingbird," *Nature*, Vol. 435, 2005, pp. 1094-1097

[4]Winter, Y., "Flight speed and body mass of nectar-feeding bats (Glossophaginae) during foraging". *Journal of Experimental Biology*, Vol. 202, pp. 1917-1930.

[5]Swartz, S.M., "Allometric patterning in the limb skeleton of bats: implications for the mechanics and energetics of powered flight," *J. Morph*., Vol. 234, 1997, pp. 277-294.

[6]Vaughan, T.A., "*The skeletal system, in The Biology of Bats*," W.A. Wimsatt, Editor, Academic Press, New York, 1970, pp. 98-139

[7]Swartz, S.M., Bennett, M.B., and Carrier, D.R., "Wing bone stresses in free flying bats and the evolution of skeletal design for flight," *Nature*, Vol. 359, 1992, pp. 726-729

[8]Swartz, S.M., et al., "Bones built to bend: In vivo loading in the distal wing of fruit bats," *Amer. Zool*., Vol. 33, 1993, pp. 75A

[9]Swartz, S.M., Bishop, K.L., Ismael-Aguirrre, M.-F., "," Akbar, Z., *Dynamic complexity of wing form in bats: implications for flight performance, in Functional and evolutionary ecology of bats* McCracken, G., and Kunz, T.H., Editors, Oxford University Press, Oxford, 2005

[10]Taylor G.K., Nudds, R.L., Thomas, A.L.R., "Flying and swimming animals cruise at a Strouhal number tuned for high power efficiency," Nature, Vol. 425, No. 16, 2003, pp. 707-711.

[11]Batchelor, G.K., *An Introduction to Fluid Dynamics*, Cambridge University Press, Cambridge, England, UK, 1967.

[12]Raffel, M., Willert, C.E., and Kompenhans, J., *Particle Image Velocimetry: a Practical Guide*, Springer-Verlag, New York, 1998.

[13]John Anderson, *Fundamentals of Aerodynamics, McGraw*-Hill Book Company, New York, 1984.